

# Fictitious Reference Iterative Tuning of Discrete-Time Model-Free Control for Tower Crane Systems

Raul-Cristian ROMAN<sup>1</sup>, Radu-Emil PRECUP<sup>1,2\*</sup>, Emil M. PETRIU<sup>3</sup>, Mihai MUNTYAN<sup>1</sup>

<sup>1</sup> Department of Automation and Applied Informatics, Politehnica University of Timisoara, Bd. 2 V. Parvan, 300223 Timisoara, Romania  
raul-cristian.roman@upt.ro, mihai.muntyan@student.upt.ro

<sup>2</sup> Center for Fundamental and Advanced Technical Research, Romanian Academy - Timisoara Branch, Bd. 24 Mihai Viteazu, 300223 Timisoara, Romania  
radu.precup@upt.ro (\*Corresponding author)

<sup>3</sup> School of Electrical Engineering and Computer Science, University of Ottawa, Ottawa, ON K1N 6N5, Canada  
petriu@uottawa.ca

**Abstract:** The purpose of this paper is to propose a novel controller that is based on a combination of two data-driven algorithms, namely the Fictitious Reference Iterative Tuning (FRIT) algorithm and the Model-Free Adaptive Control (MFC) algorithm while considering a particular form of MFC, that is the intelligent proportional-integral-derivative (iPID) controller. The main advantage of this combination is that the FRIT algorithm optimally tunes the parameters of the iPID controller by solving an optimization problem based on a metaheuristic African Vultures Optimization Algorithm (AVOA). The novel controller, referred to as the FRIT-iPID controller, is validated experimentally on a three-degree-of-freedom tower crane system laboratory equipment in the context of controlling the cart position, the arm angular position and the payload position for this system.

**Keywords:** Fictitious reference feedback tuning, Model-free control, Tower crane systems.

## 1. Introduction

In the design of control system structures, if the process model is very complex or sometimes very hard to determine, the data-driven algorithms represent a viable solution since their main feature is that the mathematical model of the process is not required in the controller tuning. Data-driven algorithms in the controller tuning require a set of input/output (I/O) data collected online or offline depending on the data-driven algorithm. In the majority of cases, the data-driven algorithms require a specific guideline in the controller tuning and design.

According to the authors' opinion, the most widely used data-driven control algorithms are Model-Free Control (MFC) (Fliess & Join, 2013), Virtual Reference Feedback Tuning (VRFT) proposed in (Campi et al., 2000) and applied to Proportional-Integral-Derivative (PID) controllers in (Formentin et al., 2019) and tower crane systems (TCS) in (Precup et al., 2021b), model-free adaptive control described in (Hou & Jin, 2014) and applied to TCS in (Roman et al., 2019a) and nonaffine nonlinear discrete-time systems in (Xiong & Hou, 2022), Iterative Feedback Tuning (IFT) suggested in (Hjalmarsson et al., 1998) and applied to TCS in (Precup et al., 2021b), and Active Disturbance Rejection Control proposed in (Gao, 2006) and applied to TCS in (Roman et al., 2021) and pressure control in (Du et al., 2023).

The main purpose of MFC reflected in algorithms for which MFC was proposed and thoroughly analyzed in (Fliess & Join, 2013) was to efficiently deal with a control system structure without using the mathematical model of the process. The main versions of MFC controllers as implementations of MFC algorithms and the most used controllers are based on classical PID controllers and are also known as intelligent Proportional-Integral-Derivative (iPID) controllers. In the past two decades since MFC was proposed it has been validated in numerous types of processes. Some representative processes where MFC algorithms are applied include: the nonlinear aerodynamic lifts of wind turbine blades (Michel et al., 2022), the two rotor aerodynamic systems, where the MFC algorithms successfully control nonlinear Multi Input-Multi Output (MIMO) processes (Roman et al., 2016a; Roman et al., 2016b; Roman et al., 2017; Roman et al., 2018a; Fliess & Join, 2022), the shape memory alloy actuators (Gédouin et al., 2008), the shape memory alloy actuators (Gédouin et al., 2008), the shape memory alloy active springs (Gédouin et al., 2011; Roman et al., 2022b), the pendulum cart system (Roman et al., 2018b) the high-performance computing systems (Guilloteau et al., 2022), the 3D cranes (Precup et al., 2021a), the TCS (Precup et al., 2021b), in avoiding cyberattacks in the multi-area power networks (Fliess et al., 2021), the myoelectric-

based controlled prosthetic hands (Precup et al., 2020), and the networking control in the industrial Internet of Things (Join et al., 2021).

An important feature of MFC algorithms is their continuous improvement by combining MFC with other data-driven algorithms with the main goal of improving the overall performance of the control system structure. One such combination involves the data-driven VRFT algorithm resulting in the MFC-VRFT combination, where the VRFT algorithm optimally determines the parameters of the MFC algorithm after considering an initial open-loop experiment (Roman et al., 2016a; Precup et al., 2021b). Another MFC improvement was made by combining the MFC algorithm with IFT resulting in the so-called P(iP)-IFT algorithm (Baciu et al., 2021) designed in the framework of optimal control.

The data-driven Fictitious Reference Iterative Tuning (FRIT) algorithm (Soma et al., 2004) is distinguished by the fact that it uses the initial I/O data collected after an initial closed-loop experiment and after several iterations returns the optimal parameters of the controller whose parameters are calculated. According to (Soma et al., 2004), FRIT gathers the advantages of two data-driven algorithms, namely VRFT and IFT since it uses an initial open-loop experiment for collecting the I/O data and the optimal parameters of the controller are returned after several iterations after solving an optimization problem. Similarly to the MFC case, the data-driven FRIT algorithm has also been applied to representative processes such as, for example, the quadrotor systems (Julkananusart & Nilkhamhang, 2015), two nonlinear systems (Wakitani & Yamamoto, 2016), the hexacopter systems (Latt et al., 2019), the Direct Current (DC) motors (Ruangurai & Silawatchananai, 2019), the systems with observation noise (Ashida, 2021), the fourth-order systems with dead time (Yahagi & Kajiwara, 2021), and the anaerobic digestion processes (Condrachi & Barbu, 2022).

This paper proposes a combination of the MFC-iPID algorithm with a FRIT algorithm. In this novel data-driven algorithm, the parameters of the MFC-iPID algorithm are determined in an optimal manner using FRIT after solving an optimization problem by making use of the metaheuristic African Vultures Optimization Algorithm (AVOA) proposed in (Abdollahzadeh et al., 2021) and applied to the optimal tuning of fuzzy controllers in (Precup et

al., 2022c). The resulting new algorithm denoted as FRIT-iPID is validated using experiments on the TCS laboratory equipment. This combination is important with respect to the state-of-the-art as it inserts a reference model (due to FRIT) in MFC.

A combination which is similar to the one proposed in this paper is reported in (Sato et al., 2022). The improvement of MFC brought about by (Sato et al., 2022) consists in the combination of iPD controllers with FRIT to optimally determine the parameters of the MFC algorithm. The advantage of the combination proposed in this paper with respect to the state-of-the-art is the optimal tuning of the free parameters of FRIT algorithms using a metaheuristic optimization algorithm.

Other notable real-time experiments on the TCS laboratory equipment of data-driven algorithms were carried out by Zhang et al. (2020), where an adaptive integral sliding mode controller was proposed, and by Zhang & Jing (2022), where a version of a model-free saturated sliding mode control technique was proposed.

The rest of the paper is structured as follows. In Section 2, the detailed nonlinear equations that describe the behavior of TCS are presented, Section 3 sets forth the new data-driven mix of discrete-time MFC-iPID and FRIT, while in Section 4 the data-driven FRIT-iPID results are highlighted. Finally, Section 5 includes the conclusions of this paper.

## 2. The Tower Crane System

The informational structure including the connection between the TC system and the personal computer through an interface is illustrated in Figure 1.

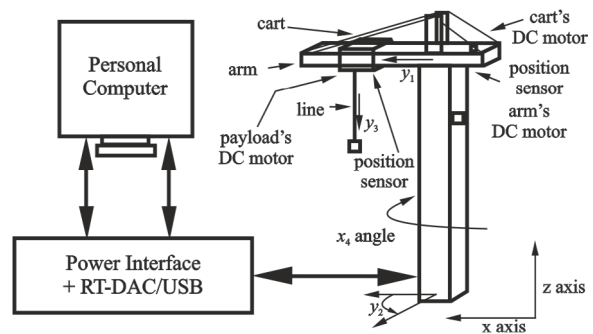


**Figure 1.** The informational structure of TCS laboratory equipment (Roman et al., 2019a; Roman et al., 2019b; Roman et al., 2020; Hedrea et al., 2021; Precup et al., 2021b; Roman et al., 2021; Precup et al., 2022a; Precup et al., 2022b; Precup et al., 2022c; Precup et al., 2022d; Roman et al., 2022a)

The mathematical model of the TCS is fully detailed in (Precup et al., 2021b; Roman et al., 2021; Precup et al., 2022a). If the time argument is omitted in order to simplify things, the state-space model of the TC system is derived from Inteco (2006) and expressed as (Precup et al., 2021b; Roman et al., 2021; Precup et al., 2022a):

$$\begin{aligned} \dot{x}_1 &= x_5, \dot{x}_2 = x_6, \dot{x}_3 = x_7, \dot{x}_4 = x_8, \dot{x}_5 = f_5(\Pi), \\ \dot{x}_6 &= f_6(\Pi), \dot{x}_7 = -(1/T_{\Sigma 1})x_7 + (k_{p1}/T_{\Sigma 1})m_1, \\ \dot{x}_8 &= -(1/T_{\Sigma 2})x_8 + (k_{p2}/T_{\Sigma 2})m_2, \dot{x}_9 = x_{10}, \\ \dot{x}_{10} &= f_{10}(\aleph), y_1 = x_3, y_2 = x_4, y_3 = x_9, \end{aligned} \quad (1)$$

where the expressions of the nonlinear functions  $f_5, f_6$  and  $f_{10}$  involved in (1) are (Precup et al., 2021b; Roman et al., 2021; Precup et al., 2022a):

$$\begin{aligned} f_5(\Pi) &= f_5(x_1, x_2, x_3, x_5, \dots, x_{10}, m_1, m_2) = \\ &[-2g \sin x_1 \cos x_2 + 4x_8x_{10} \sin x_2 - 4x_5x_{10} \\ &+ 4x_6x_8x_9 \cos^2 x_1 \cos x_2 - x_6^2x_9 \sin 2x_1 \\ &+ x_8^2x_9 \sin 2x_1 \cos^2 x_2 + 2(x_7/T_{\Sigma 1}) \sin x_1 \sin x_2 \\ &- 4x_7x_8 \cos x_1 - 2(k_{p1}/T_{\Sigma 1})m_1 \sin x_1 \sin x_2 \\ &+ 2(k_{p2}/T_{\Sigma 2})x_9m_2 \sin x_2 + 2(x_3x_8/T_{\Sigma 2}) \cos x_1 \\ &+ 2x_3x_8^2 \sin x_1 \sin x_2 - 2(k_{p2}/T_{\Sigma 2})x_3m_2 \cos x_1 \\ &- 2(x_8x_9/T_{\Sigma 2}) \sin x_2] / (2x_9), \\ f_6(\Pi) &= f_6(x_1, x_2, x_3, x_5, \dots, x_{10}, m_1, m_2) = \\ &[-(x_7/T_{\Sigma 1}) \cos x_2 - 2x_6x_{10} \cos x_1 \\ &+ 2x_5x_6x_9 \sin x_1 + (k_{p1}/T_{\Sigma 1})m_1 \cos x_2 \\ &- (k_{p2}/T_{\Sigma 2})x_9m_2 \sin x_1 \cos x_2 - x_3x_8^2 \cos x_2 \\ &+ x_8^2x_9 \cos x_1 \cos x_2 \sin x_2 - g \sin x_2 \\ &- 2x_8x_{10} \sin x_1 \cos x_2 - 2x_5x_8x_9 \cos x_1 \cos x_2 \\ &+ (x_8x_9/T_{\Sigma 2}) \sin x_1 \cos x_2] / (x_9 \cos x_1), \\ f_{10}(\aleph) &= f_{10}(x_1, x_2, x_3, x_5, \dots, x_{10}, m_1, m_2, m_3) \\ &= [(k_{p3}m_3/m_L) + x_9f_5(\Pi) \sin x_1 \cos x_2 + g \\ &+ 2x_6x_{10} \sin x_2 \cos x_1 - 2x_5x_6x_9 \sin x_1 \sin x_2 \\ &+ x_9(x_5^2 + x_6^2) \cos x_1 \cos x_2 - (\mu_L/m_L)x_{10} \\ &+ x_9f_6(\Pi) \sin x_2 \cos x_1 \\ &+ 2x_5x_{10} \sin x_1 \cos x_2] / (1 + \cos x_1 \cos x_2), \end{aligned} \quad (2)$$

and the most important variables related to the control presented in in this paper are:  $x_3$  (m)  $\in [-0.25, 0.25]$  – the first controlled output of the TC system, i.e. the cart position,  $y_1$  (m) =  $x_3$  (m),  $x$  (rad)  $\in [-1.57, 1.57]$  – the second output of the TC system, i.e. the arm angular position,  $y_2$  (rad) =  $x_4$  (rad), and  $y_3$  (m)  $\in [0.4, 0.4]$  – the third output of the TC system, i.e. the lift line position (it describes the position of the payload),  $y_3$  (m) =  $x_9$  (m). The expressions of the

nonlinearities specific to the three actuators, which are DC motors, are (Precup et al., 2021b; Roman et al., 2021; Precup et al., 2022a):

$$m_i(t) = \begin{cases} -1, & \text{if } u_i(t) \leq -u_{bi}, \\ u_i(t) + u_{ci} / (u_{bi} - u_{ci}), & \text{if } -u_{bi} < u_i(t) < -u_{ci}, \\ 0, & \text{if } -u_{ci} \leq |u_i(t)| \leq u_{ai}, \\ (u_i(t) - u_{ai}) / (u_{bi} - u_{ai}), & \text{if } u_{ai} < u_i(t) < u_{bi}, \\ 1, & \text{if } u_i(t) \geq u_{bi}, \quad i = 1 \dots 3, \end{cases} \quad (3)$$

with:  $u_1 \in [-1, 1]$  – the first control signal, i.e. the Pulse Width Modulation (PWM) duty cycle of the DC motor to control  $y_1$ ,  $u_2 \in [-1, 1]$  – the second control signal, i.e. the PWM duty cycle of the DC motor to control  $y_2$ ,  $u_3 \in [-1, 1]$  – the third control signal, i.e. the PWM duty cycle of the DC motor to control  $y_3$ , and the values of the parameters in (1), (2) and (3) are listed in (Precup et al., 2021b; Roman et al., 2021; Precup et al., 2022a). The block diagram given in Figure 1 clearly defines the reference coordinate frames focusing on the angles in different planes.

### 3. The FRIT-iPID Algorithm

First, in the current section, the discrete-time data-driven MFC-iPID algorithms are discussed and further on the novel discrete-time data-driven FRIT-iPID algorithms are detailed.

#### The discrete-time MFC-iPID algorithms

The discrete-time MFC-iPID algorithms are designed considering a discrete-time nonlinear local model of the process (Fliess & Join, 2013; Precup et al., 2021b):

$$y(k+1) = f(y(k), \dots, y(k-n_y), u(k), \dots, u(k-n_u)), \quad (4)$$

where  $k \in \mathbf{Z}$  is the discrete-time argument,  $f$  is a known nonlinear function or variable,  $u(k) \in \mathbf{R}$  is the control input,  $u(k-n_u) \in \mathbf{R}$  is the control input (or the control signal) at  $k-n_u$ ,  $y(k+1) \in \mathbf{R}$  is the controlled output, and  $y(k-n_y) \in \mathbf{R}$  is the controlled output (process output) at the  $k-n_y$  sampling interval. Therefore, the discrete-time MFC-iPID algorithm is designed to control the process model in (4) by replacing the general discrete-time local model of the process with the following first-order ultra-local model ( $n_u=0, n_y=0$ ):

$$y(k+1) = y(k) + \alpha u(k) + F(k), \quad (5)$$

where  $\alpha > 0$  is a parameter chosen by the designer such that  $\Delta y(k+1) = y(k+1) - y(k)$  and has the same order of magnitude, and  $F(k) \in \mathbf{R}$  is made from the unexpected disturbances that appear and the parts of the process that are unknown (Fliess & Join, 2013; Precup et al., 2021b).

The discrete-time MFC-iPID control law is

$$u(k) = -[\hat{F}(k) - r(k+1) + r(k) + K_1 e(k) + K_2 e(k-1) + K_3 e(k-2)] / \alpha, \quad (6)$$

where  $K_1 \in \mathbf{R}$ ,  $K_2 \in \mathbf{R}$ , and  $K_3 \in \mathbf{R}$  are the proportional, integrator, and derivative gains of the PID controller located in the MFC-iPID algorithm,  $\hat{F}(k) \in \mathbf{R}$  is the estimate of  $F(k)$  and it is calculated using the I/O data measured from the controlled process, namely

$$\hat{F}(k) = y(k) - y(k-1) - \alpha u(k-1). \quad (7)$$

The estimation error  $\delta(k)$  is:

$$\delta(k) = F(k) - \hat{F}(k) \approx 0, \quad (8)$$

and it has a negligible value,  $r(k) \in \mathbf{R}$  is the reference input (or trajectory),  $e(k)$  is the control error:

$$e(k) = r(k) - y(k). \quad (9)$$

After substituting the MFC-iPID control law with the expression in (6) into the discrete-time first-order local model of the process in (5), the dynamics equation of the closed-loop control system structure with MFC-iPID algorithm is (Fliess & Join, 2013; Precup et al., 2021b):

$$\begin{aligned} y(k+1) &= y(k) - \hat{F}(k) + r(k+1) \\ &- r(k) - K_1 e(k) - K_2 e(k-1) \\ &- K_3 e(k-2) + F(k). \end{aligned} \quad (10)$$

After substituting  $\delta(k)$  defined in (8) assuming that the norm of  $\delta(k)$  is zero, and  $e(k)$  defined in (9) into (10) the following control error dynamics associated to (10) is obtained (Fliess & Join, 2013; Precup et al., 2021b):

$$\begin{aligned} e(k+1) &+ (-1 - K_1)e(k) - K_2 e(k-1) \\ &- K_3 e(k-2) = 0. \end{aligned} \quad (11)$$

The stability of the control system with the MFC-iPID algorithm is guaranteed if all the roots of the characteristic polynomial associated to (11) are inside the unit circle.

The block diagram of the control system with discrete-time MFC-iPID algorithm is depicted in Figure 2.

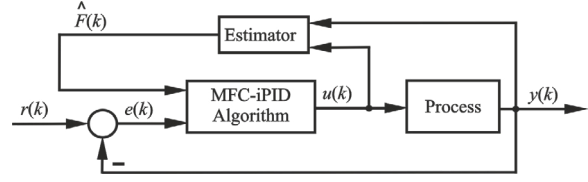


**Figure 2.** The block diagram of the control system with discrete-time MFC-iPID algorithm (Roman et al., 2016a; Roman et al., 2016b; Roman et al., 2017; Roman et al., 2018a; Roman et al., 2018b; Precup et al., 2021b; Roman et al., 2022b)

The above theory of discrete-time data-driven MFC-iPID algorithm is summarized into the following guideline that should be used for a proper and quick design of the MFC-iPID algorithm:

*Step 1.1.* Chose a value of  $\alpha > 0$  such that  $\Delta y(k+1) = y(k+1) - y(k)$  and  $\alpha u(k)$  have the same order of magnitude.

*Step 1.2.* Chose the values for  $K_1 \in \mathbf{R}$ ,  $K_2 \in \mathbf{R}$ , and  $K_3 \in \mathbf{R}$  (the parameters of the PID component in (10)) such that all the roots of the characteristic polynomial associated to (11) are inside the unit circle to guarantee the control system stability. The parameters  $K_1$ ,  $K_2$  and  $K_3$  should be chosen such that the closed-loop control system with MFC-iPID algorithms ensures a finite value for a performance index.

## The discrete-time FRIT-iPID algorithms

The following optimization problem is involved in the optimal tuning of the parameters of the PID component of the discrete-time MFC-iPID algorithm (Soma et al., 2004):

$$\begin{aligned} \Lambda^* &= \arg \min_{\Lambda} J_{FRIT}(\Lambda), \\ J_{FRIT}(\Lambda) &= \sum_{k=1}^N [y_0(\Lambda_0, k) - \tilde{y}_{\Lambda}(\Lambda, k)]^2, \end{aligned} \quad (12)$$

where  $N$  is the total number of samples that is obtained by dividing the time horizon by the number of samples,  $\Lambda_0$  is the initial parameter vector of the discrete-time data-driven MFC-iPID algorithm,  $\Lambda = [K_1 \ K_2 \ K_3]^T$  is the tunable parameter vector of discrete-time data-driven MFC-iPID algorithm,  $\Lambda^* = [K_1^* \ K_2^* \ K_3^*]^T$  is the optimal tunable parameter vector,  $y_0(\Lambda_0, k)$  is the collected output data generated after the initial experiment,  $\tilde{y}_{\Lambda}(\Lambda, k)$  is the fictitious reference model output that is computed offline knowing that (Soma et al., 2004):

$$\tilde{y}_{\Lambda}(\Lambda, k) = M(q^{-1})\tilde{r}(\Lambda, k), \quad (13)$$

where the reference model  $M(q^{-1})$  with  $q^{-1}$  as the backward shift operator is chosen by the

practitioner such that the output response of  $M(q^{-1})$  meet the performance specifications imposed to the control system. The fictitious reference input (or the virtual set-point) denoted as  $\tilde{r}(\Lambda, k)$  is computed (Soma et al., 2004):

$$\tilde{r}(\Lambda, k) = C(\Lambda, q)^{-1}u_0(\Lambda_0, k) + y_0(\Lambda_0, k), \quad (14)$$

where  $u_0(\Lambda_0, k)$  is the input data that is collected after the closed-loop real-time experiment,  $C(\Lambda, q)^{-1}$  is the inverse of the pulse transfer function of the discrete-time PID component of the MFC-iPID algorithm. The expression of the transfer function  $C(\Lambda, q)$  is:

$$C(\Lambda, q) = K_1q + K_2q^{-1} + K_3q^{-2}. \quad (15)$$

The block diagram of the control system with discrete-time FRIT-iPID algorithm is depicted in Figure 3.

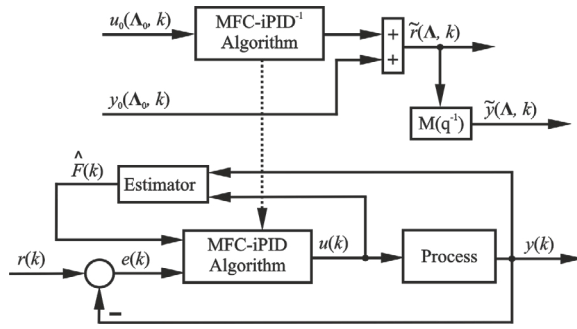


**Figure 3.** The block diagram of the control system with discrete-time FRIT-iPID algorithm

According to Soma et al. (2004), minimizing  $J_{FRIT}(\Lambda)$  in (12) is equivalent to minimizing the sum of  $(y(\Lambda, k) - M(q^{-1})r(k))^2$ , which actually guarantees model reference tracking.

The above theory of discrete-time data-driven FRIT-iPID algorithm is summarized into the following guideline that should be used for a proper and quick design of the FRIT-iPID algorithm:

*Step 2.1.* It is identical with step 1.1 for the discrete-time data-driven MFC-iPID algorithm.

*Step 2.2.* Chose the initial parameter vector  $\Lambda_0$  of the MFC-iPID algorithm so that the closed-loop control system behavior ensures a finite value of the objective function  $J_{FRIT}(\Lambda)$  in (12). This finite value is important as it avoids the need to discuss the stability of the real-world control system, which requires the process model; thus, it is a sensitive subject in data-driven control but discussed in (Precup et al., 2021b).

*Step 2.3.* The fictitious reference input  $\tilde{r}(\Lambda_0, k)$  in (14), represented in the upper side of Figure 3,

is computed by making use of  $u_0(\Lambda_0, k)$  and  $y_0(\Lambda_0, k)$ , namely the collected I/O data pair generated after the initial real-time closed-loop experiment of the control system structure with discrete-time MFC-iPID algorithm that is represented in the lower side of Figure 3.

*Step 2.4.* The reference model  $M(q^{-1})$  is chosen by the designer so that the output of  $M(q^{-1})$  fulfills the performance specifications imposed to the control system.

*Step 2.5.* The fictitious reference model output  $\tilde{y}_\Lambda(\Lambda, k)$  in (13), which is represented in the upper side of Figure 3, is computed by making use of  $M(q^{-1})$  and  $\tilde{r}(\Lambda_0, k)$ .

*Step 2.6.* The dynamic regime of the control system is set in order to allow the fair comparison of different values of the objective function in (12). The parameters of AVOA are set including the maximum number of iterations. The optimization problem in (12) is solved via metaheuristic AVOA leading to  $\Lambda^*$ . AVOA iteratively solves (12) using the stopping criterion represented by the maximum number of iterations. All these iterations are carried out off-line, without additional experiments, in terms of Figure 3 and relations (12) to (15).

## 4. The Experimental Validation

The algorithm proposed in this paper, further referred to as discrete-time FRIT-iPID algorithm, is validated in this section using experiments conducted on the TCS laboratory equipment by controlling the cart position, the arm angular position and the payload position. Therefore, three such algorithms are actually designed in this section. The discrete-time FRIT-iPID algorithms will be compared with the discrete-time MFC-iPID algorithms considering a performance index that will compute the sum of squared control errors:

$$J_{e,u}(\Lambda_\diamond) = \sum_{k=1}^N [e_1^2(\Lambda_{\diamond 1}, k) + e_2^2(\Lambda_{\diamond 2}, k) + e_3^2(\Lambda_{\diamond 3}, k)], \quad (16)$$

where  $J_{e,u}(\Lambda_\diamond)$  is the performance index used for algorithm comparison, the subscript 1 indicates the cart position, the subscript 2 indicates the arm angular position, the subscript 3 indicates the payload position, and  $\Lambda_\diamond = [\Lambda_{\diamond 1} \ \Lambda_{\diamond 2} \ \Lambda_{\diamond 3}]$  is the parameter vector of MFC-iPID (if  $\diamond = \text{MFC-iPID}$ ) and FRIT-iPID (if  $\diamond = \text{FRIT-iPID}$ ). Tracking

errors (i.e. model reference tracking errors) are not used in (16) because MFC-iPID algorithms are not designed on the basis of reference models.

In the control system structures with MFC-iPID and FRIT-iPID, the reference trajectory is composed of a separate signal for each degree of freedom of TCS:

$$\begin{aligned}
r_1(k) &= 0.15 \text{ if } k \in [0, 20/T_s], 0.1 \text{ if } \\
&k \in (20/T_s, 35/T_s], -0.05 \text{ if } \\
&k \in (35/T_s, 50/T_s], 0 \text{ if } k \in (50/T_s, 70/T_s], \\
r_2(k) &= 0 \text{ if } k \in [0, 5/T_s], 0.15 \text{ if } \\
&k \in (5/T_s, 25/T_s], -0.15 \text{ if } \\
&k \in (25/T_s, 40/T_s], 0 \text{ if } k \in (40/T_s, 70/T_s], \\
r_3(k) &= 0 \text{ if } k \in [0, 15/T_s], 0.1 \text{ if } \\
&k \in (15/T_s, 30/T_s], -0.05 \text{ if } \\
&k \in (30/T_s, 45/T_s], 0 \text{ if } k \in (45/T_s, 70/T_s],
\end{aligned} \tag{17}$$

where  $T_s = 0.01$  s is the sampling period, and the signals in (17) are filtered via discrete-time low-pass filters, one for each degree of freedom of TCS:

$$\begin{aligned}
H_{r_1}(z) &= 0.04877 / (z - 0.9512), \\
H_{r_2}(z) &= 0.0465 / (z - 0.9535), \\
H_{r_3}(z) &= 0.03278 / (z - 0.9672).
\end{aligned} \tag{18}$$

In both control system structures with MFC-iPID and FRIT-iPID algorithms the dynamic regime is characterized by the time horizon of 70 s, no additive disturbances, zero initial conditions, the nonlinear mathematical model of the TCS in (1) to (3), and the reference model composed of signals in (17) filtered via the discrete-time low-pass filters in (18).

The discrete-time MFC-iPID algorithms are designed by following the guidelines in steps 1.1 and 1.2 detailed in Section 3. First, according to step 1.1, the value of the user chosen parameter is chosen to be  $\alpha = 0.1$ . Next, according to step 1.2, the parameters  $K_1$ ,  $K_2$ , and  $K_3$  are chosen such that all the roots of the characteristic polynomial associated to (11) are inside the unit circle. This leads to:

$$\begin{aligned}
\Lambda_{0MFC_1} &= [K_{0MFC_{11}} \ K_{0MFC_{12}} \ K_{0MFC_{13}}]^T \\
&= [-0.05 \ 0.07 \ -0.05]^T, \\
\Lambda_{0MFC_2} &= [K_{0MFC_{21}} \ K_{0MFC_{22}} \ K_{0MFC_{23}}]^T \\
&= [-0.08 \ 0.014 \ -0.01]^T, \\
\Lambda_{0MFC_3} &= [K_{0MFC_{31}} \ K_{0MFC_{32}} \ K_{0MFC_{33}}]^T \\
&= [-0.124 \ -0.251 \ -0.372]^T.
\end{aligned} \tag{19}$$

The parameters in step 1.2 should be carefully chosen so that the objective function  $J_{FRIT}(\Lambda)$

defined in (12) returns a finite value for the closed-loop control system with MFC-iPID algorithms.

The discrete-time FRIT-iPID algorithms are designed by following the guidelines in steps 2.1 to 2.6 detailed in Section 3. Given the fact that step 1.1 of discrete-time MFC-iPID is identical to step 2.1 of discrete-time FRIT-iPID, the value of the user chosen parameter is  $\alpha = 5$ . In step 2.2, the initial parameter vector  $\Lambda_0$  of the MFC-iPID algorithm is picked up from (19). In step 2.3, the initial closed-loop experiment with discrete-time MFC-iPID algorithm is conducted to collect the I/O data given by the  $\{u_0(\Lambda_0, t), y_0(\Lambda_0, t)\}$  set. Further on, the fictitious reference input  $\tilde{r}(\Lambda_0, k)$  is calculated according to (14). In step 2.4, the reference model  $M(q^{-1})$  is chosen by the designer in order to embed the performance specifications in discrete time. Three reference models are set, one for each position, with the pulse transfer functions:

$$\begin{aligned}
M_1(z) &= \frac{5.813 \cdot 10^{-5} + 5.583 \cdot 10^{-5}}{z^2 - 1.886z + 0.886}, \\
M_2(z) &= \frac{1.122 \cdot 10^{-4} + 1.12 \cdot 10^{-4}}{z^2 - 1.993z + 0.993}, \\
M_3(z) &= \frac{6.399 \cdot 10^{-5} + 6.19 \cdot 10^{-5}}{z^2 - 1.905z + 0.9054}.
\end{aligned} \tag{20}$$

According to step 2.5, the fictitious reference output  $\tilde{y}_\Lambda(\Lambda, k)$  is calculated based on (13). In step 2.6, since the dynamic regime was specified above in relation to (17) and (18), some details on AVOA are given as follows:  $N_\Lambda$  is the total number of vultures or agents and each agent is assigned to a position vector  $\mathbf{X}_i(j)$

$$\begin{aligned}
\mathbf{X}_i(j) &= [x_i^1(j) \ \dots \ x_i^f(j) \ \dots \ x_i^q(j)]^T, \\
\mathbf{X}_i(j) &\in D_X \subset \mathbf{R}^q, \ i = 1 \dots N_\Lambda,
\end{aligned} \tag{21}$$

where  $x_i^f(j)$  is the position of  $i^{\text{th}}$  agent in  $f^{\text{th}}$  dimension,  $f=1 \dots q$ ,  $q$  is the dimension of the search domain  $D_X$ ,  $j$  is the index of the current iteration,  $j=1 \dots j_{\max}$ , and  $j_{\max}$  is the maximum number of iterations. Three AVOAs are actually applied, one for each degree of freedom (or position) of TCS. The AVOAs are mapped into the optimization problem in (12) in terms of

$$\begin{aligned}
q &= 3, \ \mathbf{X}_i(j) = \Lambda, \ i = 1 \dots N_\Lambda, \\
\mathbf{X}^{BV1}(j_{\max}) &= \Lambda^*,
\end{aligned} \tag{22}$$

where  $\mathbf{X}^{BV1}(j_{\max})$  is the first best solution. The parameters of the AVOAs are set as  $N_\Lambda = 7$  and  $j_{\max} = 7$ . The other parameters are  $\alpha_\Lambda = 0.8$  and  $\beta_\Lambda = 0.2$  – involved in the calculation of the probability of choosing the selected agents to

move the other agents towards one of the best solutions in each group, and  $P_1 = 0.6$ ,  $P_2 = 0.4$ ,  $P_3 = 0.6$  – thresholds in the exploration and exploitation phases; additional details are given in (Abdollahzadeh et al., 2021; Precup et al., 2022c).

The application of the three AVOAs leads to the following three solutions to the optimization problem defined in (12), one for each degree of freedom of TCS:

$$\begin{aligned} \Lambda_{\text{FRIT-iPID}_1}^* &= [K_{\text{FRIT-iPID}_{11}}^* \ K_{\text{FRIT-iPID}_{12}}^* \ K_{\text{FRIT-iPID}_{13}}^*]^T \\ &= [-0.1 \ 0.1 \ -0.02]^T, \\ \Lambda_{\text{FRIT-iPID}_2}^* &= [K_{\text{FRIT-iPID}_{21}}^* \ K_{\text{FRIT-iPID}_{22}}^* \ K_{\text{FRIT-iPID}_{23}}^*]^T \\ &= [-0.05 \ 0.021 \ 0.01]^T, \\ \Lambda_{\text{FRIT-iPID}_3}^* &= [K_{\text{FRIT-iPID}_{31}}^* \ K_{\text{FRIT-iPID}_{32}}^* \ K_{\text{FRIT-iPID}_{33}}^*]^T \\ &= [-0.091 \ -0.157 \ -0.291]^T. \end{aligned} \quad (23)$$

The experimental results for the control system structures with discrete-time MFC-iPID and FRIT-iPID algorithms for cart position, arm angular position and payload position are depicted in Figures 4-6.

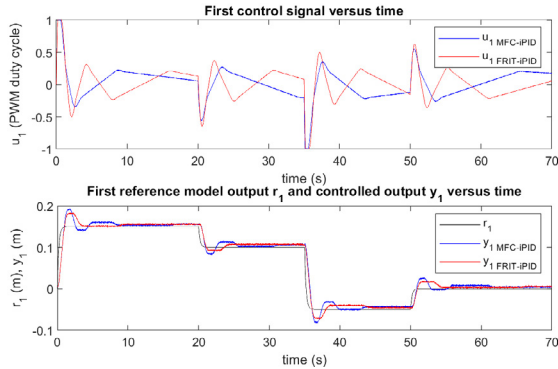


**Figure 4.** The results for cart position control systems: the first control signal versus time, the first reference model output (reference trajectory) (black) and the controlled output versus time for MFC-iPID (blue) and FRIT-iPID (red)

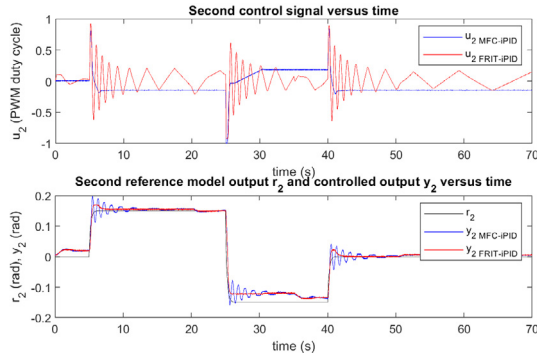


**Figure 5.** The results for arm angular position control systems: the second control signal versus time, the second reference model output (reference trajectory) (black) and the controlled output versus time for MFC-iPID (blue) and FRIT-iPID (red)

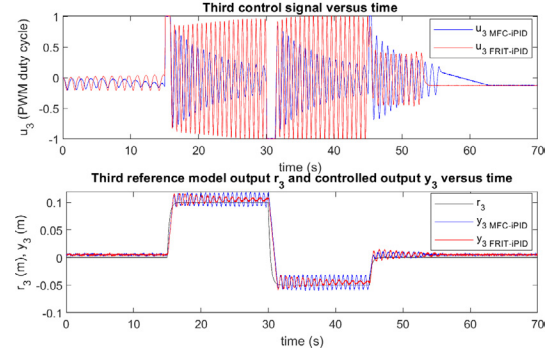


**Figure 6.** The results for payload position control systems: the third control signal versus time, the third reference model output (reference trajectory) (black) and the controlled output versus time for MFC-iPID (blue) and FRIT-iPID (red)

The evolution of the objective function in (12) minimized by using AVOA for discrete-time FRIT-iPID algorithm dedicated to arm angular position control is illustrated in Figure 7. The value of  $J_{\text{FRIT}}(\Lambda) = J_{\text{FRIT}}(\Lambda_{0\text{MFC}_2})$  related to (19) is not represented in Figure 7 because the initial step of AVOA carries out the random initialization of the position vectors of the population of agents such that they belong to the search domain.

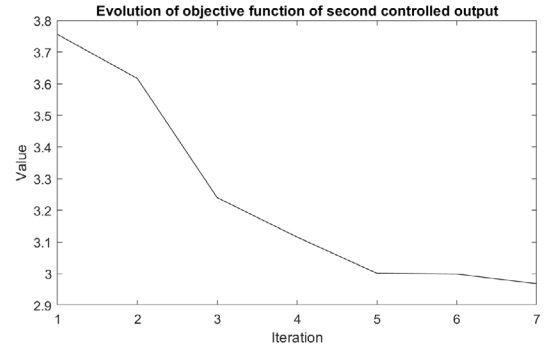


**Figure 7.** The evolution of the objective function in (12) for the discrete-time FRIT-iPID algorithm for arm angular position control

The values of the performance index  $J_{e,u}(\Lambda_\diamond)$  defined in (16) for the control systems with the discrete-time FRIT-iPID algorithms and the discrete-time MFC-iPID algorithms are given in Table 1.

**Table 1.** The average and variance of performance index  $J_{e,u}(\Lambda_\diamond)$  values after ten real-time experiments for MIMO TCS

	MFC-iPID	FRIT-iPID
Average of $J_{e,u}(\Lambda_\diamond)$	3.9826	2.9683
Variance of $J_{e,u}(\Lambda_\diamond)$	$8.5954 \times 10^{-5}$	$8.9004 \times 10^{-5}$

The values in Table 1 correspond to ten experiments repeated in the same conditions (i.e. dynamic regime). The goal of determining the average and variance of the values of  $J_{e,u}(\Lambda_\diamond)$  is to mediate the

random unexpected disturbances that can appear during the real-time experiments and reflect the effects of the random parameters specific to AVOA.

The graphical results displayed in Figures 4–6 and the performance index values in Table 1 highlight that after seven iterations the discrete-time FRIT-iPID algorithms exhibit a significant improvement since the performance is approximately 1.34 times better than that of the discrete-time MFC-iPID algorithms. Different results would have been obtained if different objectives were defined in reducing the control error or reducing the (reference model) tracking error contexts. Since the discrete-time FRIT-iPID algorithms perform better for the complex process represented by TCS, this result is encouraging for other relevant applications such as, for example, human well-being and resilience (Filip, 2021), fuzzy logic in IoT and intelligent space (Hvizdoš et al., 2015), tensor product-based model transformation (Baranyi et al., 2004; Hedrea et al., 2021), evolutionary multitasking (Osaba et al., 2021), evolving systems (Blažič et al., 2014), electric vehicles (Johanyák, 2017), and vertical take-off and landing drones (Ucgun et al., 2022).

## 5. Conclusion

The current paper proposed a new combination of two discrete-time data-driven algorithms, namely FRIT and MFC-iPID, referred to as discrete-time data-driven FRIT-iPID algorithm. The AVOA algorithm was tested through experiments by controlling the cart, arm angular and payload

positions of the TCS laboratory equipment, and three data-driven control algorithms were implemented.

The main feature of FRIT-iPID is that FRIT iteratively determines the optimal parameters of the PID component of discrete-time MFC-iPID making use only of the I/O data collected after a closed-loop initial experiment by solving an optimization problem via metaheuristic AVOA. The initial FRIT (Soma et al., 2004), where just a one-shot experiment is conducted, and then off-line Gauss-Newton optimization computations are carried out, is replaced with AVOA in this paper. The weak point of the AVOA-based discrete-time FRIT-iPID algorithm is that several experiments are needed to mitigate the effects of the random parameters specific to AVOA. In the case presented in this paper the objective functions returned acceptable values after seven iterations.

Future work will aim at the validation of the proposed discrete-time FRIT-iPID algorithm using experiments that will be conducted on other laboratory equipment. Future work will also include the improvement of data-driven algorithms in order to further enhance the performance of the control systems' structure.

## Acknowledgements

The research reported in this paper was supported by a grant from the Romanian Ministry of Education and Research, CNCS - UEFISCDI, project number PN-III-P4-ID-PCE-2020-0269, and by the NSERC of Canada.

## REFERENCES

- Abdollahzadeh, B., Gharehchopogh, F. S. & Mirjalili, S. (2021) African Vultures Optimization Algorithm: A New Nature-inspired Metaheuristic Algorithm for Global Optimization Problems. *Computers & Industrial Engineering*. 158, 1-37.
- Ashida, Y. (2021) Comparison of Regression Methods on Data-driven Controller Design for Systems with Observation Noise. In: *Proceedings of 20<sup>th</sup> International Symposium on Communications and Information Technologies, Tottori, Japan*. pp. 55-58.
- Baciu, A., Lazar, C. & Caruntu, C.-F. (2021) Iterative Feedback Tuning of Model-free Controllers. In: *Proceedings of 25<sup>th</sup> International Conference on System Theory, Control and Computing, Iasi Romania*. pp. 467-472.
- Baranyi, P., Korondi, P., Patton, R. J. & Hashimoto, H. (2004) Trade-off Between Approximation Accuracy and Complexity for TS Fuzzy Models. *Asian Journal of Control*. 6(1), 21-33.
- Blažič, S., Dovžan, D. & Škrjanc, I. (2014) Cloud-based Identification of an Evolving System With Supervisory Mechanisms. In: *Proceedings of 2014 IEEE International Symposium on Intelligent Control, Antibes, France*. pp. 1906-1911.
- Campi, M. C., Lecchini, A. & Savaresi, S. M. (2000) Virtual Reference Feedback Tuning (VRFT): a New Direct Approach to the Design of Feedback Controllers. In: *Proceedings of 39<sup>th</sup> Conference on Decision and Control, Sydney, Australia*. pp. 623-628.
- Condrachi, L. & Barbu, M. (2022) Anaerobic Digestion Processes Controller Tuning Using Fictitious Reference Iterative Method. *IFAC-PapersOnLine*. 55(7), 453-458.
- Du, Y.-W., Cao, W.-H. & She, J.-H. (2023) Analysis and Design of Active Disturbance Rejection Control

- With an Improved Extended State Observer for Systems With Measurement Noise. *IEEE Transactions on Industrial Electronics*. 70(1), 855-865.
- Filip, F. G. (2021) Automation and Computers and Their Contribution to Human Well-being and Resilience. *Studies in Informatics and Control*. 30(4), 5-18, DOI: 10.24846/v30i4y202101.
- Fliess, M. & Join, C. (2013) Model-free Control, *International Journal of Control*. 86(12), 2228-2252.
- Fliess, M., Join, C. & Sauter, D. (2021) Defense Against DoS and Load Altering Attacks via Model-free control: A Proposal for a New Cybersecurity Setting. In: *Proceedings of 5<sup>th</sup> International Conference on Control and Fault-Tolerant Systems, Saint-Raphael, France*. pp. 58-65.
- Fliess, M. & Join, C. (2022) An Alternative to Proportional-Integral and Proportional-Integral-Derivative Regulators: Intelligent Proportional-Derivative Regulators. *International Journal of Robust and Nonlinear Control*. 32(18), 9612-9524.
- Formentin, S., Campi, M. C., Caré, A. & Savaresi, S. M. (2019) Deterministic Continuous-time Virtual Reference Feedback Tuning (VRFT) with Application to PID Design. *Systems and Control Letters*. 127, 25-34.
- Gao, Z. (2006) Active Disturbance Rejection Control: a Paradigm Shift in Feedback Control System Design. In: *Proceedings of 2006 American Control Conference, Minneapolis, MN, USA*. pp. 2399-2405.
- Gédouin, P.-A., Join, C., Delaleau, E., Bourgeot, J.-M., Chirani, S. A. & Calloch, S. (2008) Model-free Control of Shape Memory Alloys Antagonistic Actuators. *IFAC Proceedings Volumes*. 41(2), 4458-4463.
- Gédouin, P.-A., Delaleau, E., Bourgeot, J.-M., Join, C., Chirani, S. A. & Calloch, S. (2011) Experimental Comparison of Classical PID and Model-free Control: Position Control of a Shape Memory Alloy Active Spring. *Control Engineering Practice*. 19(5), 433-441.
- Guilloteau, Q., Robu, B., Join, C., Fliess, M., Rutten, E. & Richard, O. (2022) Model-free Control for Resource Harvesting in Computing Grids. In: *Proceedings of 2022 IEEE Conference on Control Technology and Applications, Trieste, Italy*. pp. 384-390.
- Hedrea, E.-L., Precup, R.-E., Roman, R.-C. & Petriu, E. M. (2021) Tensor Product-based Model Transformation Approach to Tower Crane Systems Modeling. *Asian Journal of Control*. 23(3), 1313-1323.
- Hjalmarsson, H., Gevers, M., Gunnarsson, S. & Lequin, O. (1998) Iterative Feedback Tuning: Theory and Applications. *IEEE Control Systems Magazine*. 18(4), 24-41.
- Hou, Z.-S. & Jin, S.-T. (2014) *Model Free Adaptive Control. Theory and Applications*. (1<sup>st</sup> ed.) Boca Raton, FL, CRC Press, Taylor & Francis.
- Hvizdoš, J., Vaščák, J. & Březina, A. (2015) Object Identification and Localization by Smart Floors. In: *Proceedings of IEEE 19<sup>th</sup> International Conference on Intelligent Engineering Systems, Bratislava, Slovakia*. pp. 113-117.
- Inteco (2006) *Tower Crane, User's Manual*, Krakow, Inteco Ltd.
- Johanyák, Z. C. (2017) A Modified Particle Swarm Optimization Algorithm for the Optimization of a Fuzzy Classification Subsystem in a Series Hybrid Electric Vehicle. *Tehnički vjesnik*. 24(2), 295-301.
- Join, C., Fliess, M., & Chaxel, F. (2021) Model-free Control as a Service in the Industrial Internet of Things: Packet Loss and Latency Issues via Preliminary Experiments. In: *Proceedings of 5<sup>th</sup> International Conference on Control and Fault-Tolerant Systems, Saint-Raphael, France*. pp. 299-306.
- Julkananusart, A. & Nilkhamhang, I. (2015) Quadrotor Tuning for Attitude Control Based on Double-loop PID Controller Using Fictitious Reference Iterative Tuning (FRIT). In: *Proceedings of 41<sup>st</sup> Annual Conference of the IEEE Industrial Electronics Society, Yokohama, Japan*. pp. 004865-004870.
- Latt, Z. K. K., Si, H. & Kaneko, O. (2019) Controller Parameter Tuning of a Hexacopter with Fictitious Reference Iterative Tuning. In: *Proceedings of 2019 SICE International Symposium on Control Systems, Kumamoto, Japan*. pp. 96-101.
- Michel, L., Neunaber, I., Mishra, R., Braud, C., Plestan, F., Barbot, J.-P., Boucher, X., Join, C. & Fliess, M. (2022) Model-free Control of the Dynamic Lift of a Wind Turbine Blade Section: Experimental Results. *Journal of Physics: Conference Series*. 2265, paper 032068.
- Osaba, E., Del Ser, J., Martinez, A. D., Lobo, J. L. & Herrera, F. (2021) AT-MFCGA: An Adaptive Transfer-guided Multifactorial Cellular Genetic Algorithm for Evolutionary Multitasking. *Information Sciences*. 570, 577-598.
- Precup, R.-E., Roman, R.-C., Teban, T.-A., Albu, A., Petriu, E. M. & Pozna, C. (2020) Model-free Control of Finger Dynamics in Prosthetic Hand Myoelectric-based Control Systems. *Studies in Informatics and Control*. 29(4), 399-410, DOI: 10.24846/v29i4y202002.
- Precup, R.-E., Roman, R.-C., Hedrea, E.-L., Petriu, E. M. & Bojan-Dragos, C.-A. (2021a) Data-driven Model-free Sliding Mode and Fuzzy Control with Experimental Validation. *International Journal of Computers Communications and Control*. 16(1), 1-17.
- Precup, R.-E., Roman, R.-C. & Safaei, A. (2021b) *Data-driven Model-free Controllers*. (1<sup>st</sup> ed.) Boca Raton, FL, CRC Press, Taylor & Francis.
- Precup, R.-E., Hedrea, E.-L., Roman, R.-C., Petriu, E. M., Bojan-Dragos, C.-A. & Szedlak-Stinean, A.-I. (2022a) GWO-based Performance Improvement of PD-type Iterative Learning Fuzzy Control of Tower Crane Systems. In: *Proceedings of 2022 IEEE 31<sup>st</sup> International Symposium on Industrial Electronics, Anchorage, AK, USA*. pp. 1041-1046.
- Precup, R.-E., Hedrea, E.-L., Roman, R.-C., Petriu, E. M., Bojan-Dragos, C.-A., Szedlak-Stinean, A.-I. & Hedrea, I.-C. (2022b) Evolving Fuzzy and Tensor Product-based Models for Tower Crane Systems. In: *Proceedings of 48<sup>th</sup> Annual Conference of the IEEE Industrial Electronics Society, Bruxelles, Belgium*. pp. 1-6.

- Precup, R.-E., Hedrea, E.-L., Roman, R.-C., Petriu, E. M., Bojan-Dragos, C.-A., Szedlak-Stinean, A.-I. & Paulescu, F.-C. (2022c) AVOA-Based Tuning of Low-cost Fuzzy Controllers for Tower Crane Systems. In: *Proceedings of 2022 IEEE International Conference on Fuzzy Systems, Padua, Italy*. pp. 1-8.
- Precup, R.-E., Roman, R.-C., Hedrea, E.-L., Bojan-Dragos, C.-A., Damian, M.-M. & Nedelcea M.-L. (2022d) Performance Improvement of Low-Cost Iterative Learning-Based Fuzzy Control Systems for Tower Crane Systems. *International Journal of Computers Communications & Control*. 17(1), 1-18.
- Roman, R.-C., Radac, M.-B. & Precup, R.-E. (2016a) Mixed MFC-VRFT Approach for a Multivariable Aerodynamic System Position Control. In: *Proceedings of 2016 IEEE International Conference on Systems, Man, and Cybernetics, Budapest, Hungary*. pp. 002615-002620.
- Roman, R.-C., Radac, M.-B. & Precup, R.-E. (2016b) Multi-Input-Multi-Output System Experimental Validation of Model-free Control and Virtual Reference Feedback Tuning Techniques. *IET Control Theory & Applications*. 10(12), 1395-1403.
- Roman, R.-C., Precup, R.-E. & Radac, M.-B. (2017) Model-Free Fuzzy Control of Twin Rotor Aerodynamic Systems. In: *Proceedings of 2017 25<sup>th</sup> Mediterranean Conference on Control and Automation, Valetta, Malta*. pp. 559-564.
- Roman, R.-C., Precup, R.-E. & David R.-C. (2018a) Second Order Intelligent Proportional-Integral Fuzzy Control of Twin Rotor Aerodynamic Systems. *Proceedings of Procedia Computer Science*. 139, 372-380.
- Roman, R.-C., Radac, M.-B., Tureac, C., & Precup, R.-E. (2018b) Data-Driven Active Disturbance Rejection Control of Pendulum Cart Systems. In: *2018 IEEE Conference on Control Technology and Applications, Copenhagen, Denmark*. pp. 933-938.
- Roman, R.-C., Precup, R.-E., Petriu, E. M., Hedrea, E.-L., Bojan-Dragos, C.-A. & Radac, M.-B. (2019a) Model-free Adaptive Control With Fuzzy Component for Tower Crane Systems. In: *Proceedings of 2019 IEEE International Conference on Systems, Man and Cybernetics, Bari, Italy*. pp. 1384-1389.
- Roman, R.-C., Precup, R.-E., Bojan-Dragos, C.-A. & Szedlak-Stinean, A.-I. (2019b) Combined Model-Free Adaptive Control with Fuzzy Component by Virtual Reference Feedback Tuning for Tower Crane Systems. In: *Proceedings of Procedia Computer Science 162, Granada, Spain*. pp. 267-274.
- Roman, R.-C., Precup, R.-E., Petriu, E. M., David, R.-C., Hedrea, E.-L. & Szedlak-Stinean, A.-I. (2020) First-Order Active Disturbance Rejection-Virtual Reference Feedback Tuning Control of Tower Crane Systems. In: *Proceedings of 2020 24<sup>th</sup> International Conference on System Theory, Control and Computing, Cheile Gradistei, Romania*. pp. 137-142.
- Roman, R.-C., Precup, R.-E. & Petriu, E. M. (2021) Hybrid Data-driven Fuzzy Active Disturbance Rejection Control for Tower Crane Systems. *European Journal of Control*, 58, 373-387.
- Roman, R.-C., Precup, R.-E., Hedrea, E.-L., Preitl, S., Zamfirache I. A., Bojan-Dragos, C.-A. & Petriu E. M. (2022a) Iterative Feedback Tuning Algorithm for Tower Crane Systems. In: *Proceedings of Procedia Computer Science 199, Chengdu, China*. pp. 157-165.
- Roman, R.-C., Precup, R.-E., Preitl, S., Bojan-Dragos, C.-A., Szedlak-Stinean, A.-I. & Hedrea, E.-L. (2022b) Data-Driven Control Algorithms for Shape Memory Alloys. In: *Proceedings of 2022 IEEE Conference on Control Technology and Applications, Trieste, Italy*. pp. 1306-1312.
- Ruangurai, P. & Silawatchananai, C. (2019) Implementation of PSO Based Fictitious Reference Iterative Tuning to Embedded System. In: *Proceedings of 2019 7<sup>th</sup> International Conference on Control, Mechatronics and Automation, Delft, Netherlands*. pp. 365-369.
- Sato, T., Miyake, S. & Kaneko, O. (2022) An Extension of Intelligent PID Control System to I-PD Typed Control System and Parameter Tuning by FRIT. *IEEE Transactions on Electronics, Information and Systems*. 142(3), 299-306.
- Soma, S., Kaneko, O., & Fujii, T. (2004) A New Method of Controller Parameter Tuning Based on Input-Output Data – Fictitious Reference Iterative Tuning (FRIT). *IFAC Proceedings Volumes*. 37(12), 789-794.
- Ucgun, H., Okten, I., Yuzgec, U. & Kesler, M. (2022) Test Platform and Graphical User Interface Design for Vertical Take-off and Landing Drones. *Romanian Journal of Information Science and Technology*. 25(3-4), 350-367.
- Wakitani, S. & Yamamoto, T. (2016) A Learning Algorithm for a Data-driven Controller Based on Fictitious Reference Iterative Tuning. In: *Proceedings of 2016 International Joint Conference on Neural Networks, Vancouver, BC, Canada*. pp. 4908-4913.
- Xiong, S.-S. & Hou, Z.-S. (2022) Model-free Adaptive Control for Unknown MIMO Nonaffine Nonlinear Discrete-time Systems with Experimental Validation. *IEEE Transactions on Neural Networks and Learning Systems*. 33(4), 1727-1739.
- Yahagi, S. & Kajiwara, I. (2021) Direct Tuning of PID Controller and Reference Model With Input Constraint. In: *Proceedings of 2021 21<sup>st</sup> International Conference on Control, Automation and Systems, Jeju, Republic of Korea*. pp. 1424-1429.
- Zhang, M., Zhang, Y., Ouyang, H., Ma, C. & Cheng, X. (2020) Adaptive Integral Sliding Mode Control with Payload Sway Reduction for 4-DOF Tower Crane Systems. *Nonlinear Dynamics*. 99, 2727-2741.
- Zhang, M. & Jing, Z. (2022) Model-free Saturated PD-SMC Method for 4-DOF Tower Crane Systems. *IEEE Transactions on Industrial Electronics*. 69(10), 10270-10280.